

PAPER • OPEN ACCESS

Numerical modeling of Liesegang structures formation process under an electric field influence

To cite this article: V Kireev *et al* 2019 *J. Phys.: Conf. Ser.* **1391** 012120

View the [article online](#) for updates and enhancements.

You may also like

- [Surface conductivity of insulators: two-dimensional cylindrical symmetry](#)
S R Holcombe, J Liesegang and E R Smith
- [On the behaviour of the Cd d bands in Au, Ag and Hg alloys](#)
J A Nicholson, R C G Leckey, J D Riley et al.
- [Crystal-field splitting in strongly ionic solids studied by photoelectron spectroscopy](#)
R T Poole, J D Riley, D R Williams et al.



ECS The Electrochemical Society
Advancing solid state & electrochemical science & technology

242nd ECS Meeting

Oct 9 – 13, 2022 • Atlanta, GA, US

Early hotel & registration pricing ends September 12

Presenting more than 2,400 technical abstracts in 50 symposia

The meeting for industry & researchers in
BATTERIES
ENERGY TECHNOLOGY
SENSORS AND MORE!

 Register now!

  **ECS Plenary Lecture featuring M. Stanley Whittingham,**
Binghamton University
Nobel Laureate –
2019 Nobel Prize in Chemistry



Numerical modeling of Liesegang structures formation process under an electric field influence

V Kireev¹, B Shalabayeva², N Jaichibekov², A Nizamova³, Z Kozhabay²

¹Department of applied physics, Bashkir State University,
32 Zaki Validi str., Ufa 450076, Russia

²Faculty of mechanics and mathematics, L.N. Gumilyov Eurasian National University,
13 Kazhimukan str., Nur-Sultan 010008, Qazaqstan

³Laboratory of mechanics of multiphase systems, Mavlutov Institute of Mechanics
71 Prospekt Oktyabrya, Ufa 450054, Russia

E-mail: kireev@anrb.ru

Abstract. In the present paper the formation of Liesegang structures, i.e. the process of periodic deposition with the mutual diffusion of two reacting chemicals in the presence of an external constant electric field, is studied using numerical modeling. The mathematical model of the process consists of three differential equations of diffusion-reaction for the concentrations of the initial components and the resulting precipitate. The kinetics of sedimentation is described in accordance with the Ostwald's supersaturation theory. The equations of the mathematical model in one-dimensional and two-dimensional statements were solved numerically using the control volume method using computer code written by the authors in the C++ language. As a result of numerical simulation in the absence of an electric field, periodic structures were obtained formed of the precipitate, which qualitatively corresponds to the patterns observed in the experiments. It is shown that numerically obtained Liesegang rings satisfy the well-known laws: the ratio of the distances to neighbouring rings remains constant and there is a power dependence between the distances to the rings and the time of their formation. The influence of the ratio of the concentration of the starting substances and the electric field strength on the nature of the structures formed is investigated. It also has been shown that an increase in the electric field strength leads to an increase in the number of structures formed.

1. Introduction

Oscillatory chemical reactions, in which the concentrations of reacting substances change periodically, have been the subject of study by scientists of various specialties for more than one hundred years: chemists, physicists, biologists, geologists, physicians, mathematicians. The best-known examples of oscillatory chemicals reactions are Bray-Liebhafsky reaction (1921), Belousov-Zhabotinsky reaction (1958) and Briggs-Rauscher reaction (1972). Liesegang rings (or layers), representing spatial periodic structures, were first discovered by the German chemist Raphael Edward Liesegang in 1896 [1], but a theory has not yet been created that can explain all the mechanisms underlying this periodic reaction. Further theoretical and experimental study of the patterns of formation of Liesegang structures can, in particular, contribute to a deeper understanding of the characteristics of sedimentation in various technological processes in petrochemical production.



2. Mathematical model

Let's consider one-dimensional process of periodic precipitation as a result of the following chemical reactions:



The schematic representation of the domain in consideration, the coordinate system and the key legend are shown in figure 1. The substance A diffuses into gel saturated with the substance B, reacts with it and gives the product C, that can precipitate as D.

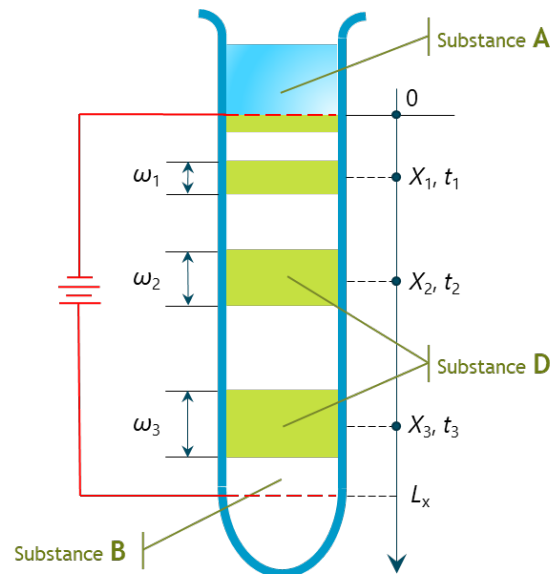


Figure 1. To the problem statement.

The following mathematical model consisting of four transient reaction-diffusion equations corresponds the reaction scheme (1):

$$\begin{aligned} \frac{\partial a}{\partial t} &= D_A \frac{\partial^2 a}{\partial x^2} - z_A E \frac{\partial a}{\partial x} - k_1 ab, \\ \frac{\partial b}{\partial t} &= D_B \frac{\partial^2 b}{\partial x^2} - z_B E \frac{\partial b}{\partial x} - k_1 ab, \\ \frac{\partial c}{\partial t} &= D_C \frac{\partial^2 c}{\partial x^2} + k_1 ab - k_2 P(c, d), \\ \frac{\partial d}{\partial t} &= k_2 P(c, d), \end{aligned} \quad (2)$$

where a , b , c , and d are concentrations of the substances A, B, C, and D; D_A , D_B , and D_C are the diffusion coefficients of the substances A, B, and D; k_1 and k_2 are the chemical rate constants for the reaction (1); z_A and z_B are the charges of the ions A^+ and B^- ; E is the constant electric field strength. It is supposed that the electric field doesn't influence on the molecules of the substances C and D and also the precipitated substance D is immobile and doesn't diffuse.

There exists a number of theories describing the precipitation kinetics and giving the expressions for the function $P(c, d)$. Following the Keller-Rubinow theory [2] this function is adopted as

$$P(c,d) = \begin{cases} 0, & \text{if } c < C_s \text{ \& } d = 0 \\ (c - C_*) \cdot \Theta(c - C_*), & \text{otherwise} \end{cases} \quad (3)$$

where C_* is the saturation concentration; C_s is the supersaturation concentration; Θ is the Heaviside function.

The equation (3) describes the simple assumption concerning supersaturation nucleation and postulates that if concentration of the substance D is zero (that is no precipitations at the point in consideration) and concentration of the substance C is less than the supersaturation concentration C_s then the precipitation reaction doesn't proceed. Otherwise, if there are any precipitations at the point or the substance C concentration exceeds the saturation concentration C_* precipitations occur but only in the case when the substance C concentration is greater than the supersaturation concentration $C_s > C_*$.

To complete the mathematical model of the process one has to set the initial conditions

$$a(0,x) = 0, \quad b(0,x) = b_0, \quad c(0,x) = 0, \quad d(0,x) = 0 \quad (4)$$

and the boundary conditions

$$a(t,0) = a_0, \quad \left. \frac{\partial b}{\partial x} \right|_{x=0} = \left. \frac{\partial c}{\partial x} \right|_{x=0} = 0, \quad \left. \frac{\partial a}{\partial x} \right|_{x=L_x} = \left. \frac{\partial b}{\partial x} \right|_{x=L_x} = \left. \frac{\partial c}{\partial x} \right|_{x=L_x} = 0. \quad (5)$$

3. Numerical model

Numerical solution of the system of partial differential equations (2) with initial and boundary conditions (4)-(5) is performed using the finite volume method [3]. Let's illustrate the procedure for obtaining the discrete analog of differential equation on the example of the first equation in system (2).

According to the finite volume method paradigm one has to integrate all the terms in the differential equation over the typical inner control volume (shown in figure 2 in red color) and over the time interval (to avoid further confusion the concentration of the substances A and B are denoted as α and β in the current section):

$$\int_w^e \int_t^{t+\Delta t} \frac{\partial \alpha}{\partial t} dt dx = \int_t^{t+\Delta t} \int_w^e D_A \frac{\partial^2 \alpha}{\partial x^2} dx dt - \int_t^{t+\Delta t} \int_w^e z_A E \frac{\partial \alpha}{\partial x} dx dt - \int_t^{t+\Delta t} \int_w^e k_1 \alpha \beta \cdot dx dt. \quad (6)$$

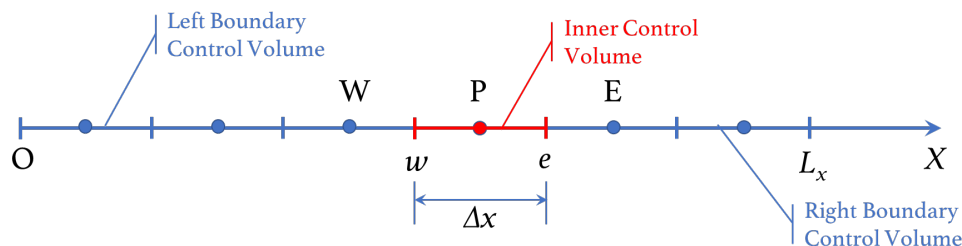


Figure 2. Discretisation of the computational domain.

After performing all the computations one can express the discrete equation in the standard form as

$$a_p \alpha_p = a_w \alpha_w + a_e \alpha_e + b, \quad (7)$$

where a_p , a_w , a_e and b are the coefficients whose expressions for inner and boundary control volumes are summarized in the table 1. The superscript "0" denotes the known value of the variable at the previous time step and the new quantity $\alpha_p^0 = \Delta x / \Delta t$ is introduced.

Table 1. The coefficients of the discrete equation

	Left Boundary Control Volume	Inner Control Volumes	Right Boundary Control Volume
a_W	0	$D_A / \Delta x + z_A E / 2$	$D_A / \Delta x + z_A E / 2$
a_E	$D_A / \Delta x - z_A E / 2$	$D_A / \Delta x - z_A E / 2$	0
a_p	$a_W + a_E + a_p^0 + 2D_A / \Delta x + z_A E / 2$	$a_W + a_E + a_p^0$	$a_W + a_E + a_p^0$
b	$a_p^0 \alpha_p^0 - k_1 \alpha_p^0 \beta_p^0 + (2D_A / \Delta x + z_A E) \alpha_0$	$a_p^0 \alpha_p^0 - k_1 \alpha_p^0 \beta_p^0$	$a_p^0 \alpha_p^0 - k_1 \alpha_p^0 \beta_p^0$

The similar discrete equations are obtained for the concentrations of the substances B, C and D. The resulting systems of linear algebraic equations for concentration of each substance are solved sequentially at every time step using tridiagonal matrix algorithm (TDMA).

4. The results of numerical modeling

The following non-dimensional parameters have been chosen for numerical modeling:

$$D_A = D_B = D_C = 0.001, \quad k_1 = k_2 = 50, \quad C_* = 0.2, \quad C_s = 0.8, \quad (8)$$

$$a_0 = 10, \quad b_0 = 10, \quad L_x = 1.5, \quad \Delta x = 0.015, \quad \Delta t = 0.001, \quad z_A = 1, \quad z_B = -1.$$

In the figure 3 spatial distributions of concentrations of all the substances at the same time ($t = 100$) under the influence of electric fields of different strengths are shown. The red lines correspond to the absence of electric field ($E = 0$). In this case only two bands at points $x = 0.0675$ and $x = 0.2475$ have been formed at the time in question. The presence of an electric field with relatively small strength $E = 0.001$ (blue lines in the figure 3) changes the picture significantly. Since the ions of the substance A have a positive charge, the forces acting on them from the electric field contribute to the diffusion process and therefore the substance A penetrates into the gel more quickly and to the greater distance. This leads to an increase in the number of bands formed to four, and the last band begins to form at the point $x = 0.7425$. A further increase in the electric field strength enhances the phenomena described. For the electric field strength $E = 0.005$ (green lines in the figure 3) one can see that the distance between the bands decreases, the number of bands doubles and reaches eight. It should also be noted that the amount of precipitate formed (which is characterized by the amplitude of the corresponding “peak” on the plot) is significantly less than for the other two cases. Some interesting observations can be made when considering the graph for the concentration of the substance C. For the red line, the concentration of the substance C near the point $x = 0.75$ approaches the supersaturation concentration $C_s = 0.8$. This means that sedimentation will occur at this point at subsequent points in time and another band will be formed. On the contrary, for the blue line the concentration near the point $x = 0.75$ decreased to the saturation concentration $C_* = 0.2$, i.e. sedimentation has already occurred and the amount of sediment at this point will increase subsequently.

Let introduce two new quantities: t_n is the time when the n -th band has been formed, and x_n is the distance from the origin ($x = 0$) to the n -th band, i.e. the x -coordinate of the n -th “peak”. The well-known fact, confirmed by numerous experimental observations and theoretical considerations, is that the quantities x_n and t_n obey two relations: the so-called “spacing” law

$$x_{n+1} = P \cdot x_n, \quad P > 1 \quad (9)$$

and “time” law

$$t_n = (x_n / \alpha)^2, \quad \alpha > 0. \quad (10)$$

In the figure 4 two plots are represented: the left plot (a) shows the position of the $(n+1)$ -th band x_{n+1} versus the position of the n -th band x_n , and the right one (b) shows the dependence of $\sqrt{t_n}$ on x_n . Different color of the small circles refer to different electric field strengths.

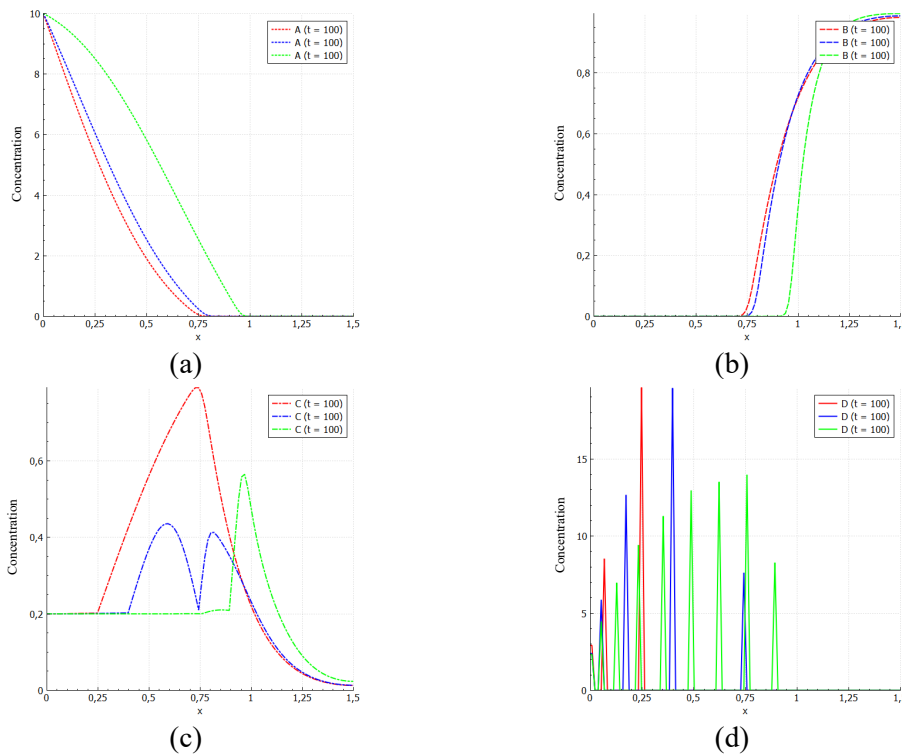


Figure 3. Spatial distribution of concentrations of substances A (a), B (b), C (c), and D (d) at the same time under the influence of different electric fields: 0 (red line), 0.001 (blue line), 0.005 (green line).

From the figure 4 (a) it is clearly seen that the “spacing” law is fulfilled both in the absence of an electric field and in its presence: the dependence x_{n+1} on x_n remains linear. An increase of the electric field strength leads to a decrease in the inclination angle of the corresponding straight line, and the coefficient P then tends to unity. In the limit, for very large values of the electric field strength, the bands will not form, and precipitations will form evenly along the entire region length.

The figure 4 (b) shows that the “time” law (10) is executed only at the small values of the electric field strength up to $E = 0.001$. With further increase E , the dependence $\sqrt{t_n}$ on x_n becomes nonlinear and can be approximated by a quadratic dependence of the form (see also [4])

$$x_n = \alpha_1(t_n)^{1/2} + \alpha_2 \cdot t_n + \alpha_3, \tag{11}$$

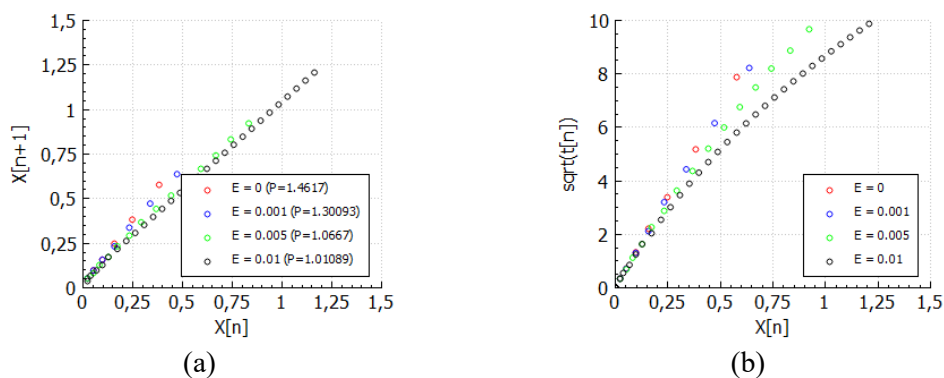


Figure 4. Spacing (a) and time (b) laws under electric field influence.

All previous numerical results were obtained for the case when the electric field strength has positive values. The figure 5 represents precipitation patterns under the influence of different direction electric fields. Analysis of the data in this figure shows that, depending on the direction of the electric field, the number of bands may either increase (for positive values E) or decrease (for negative values E) as compared to the case of the absence of an electric field.

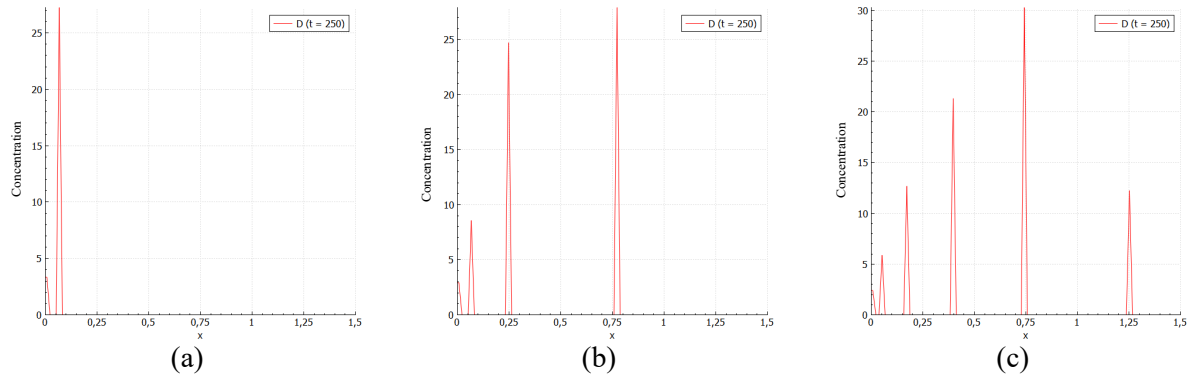


Figure 5. Precipitation patterns under the influence of different direction electric fields: (a) $E = -0.001$, (b) $E = 0$, (c) $E = 0.001$.

5. Conclusion

It is shown that numerically obtained Liesegang rings satisfy in the absence of an electric field the well-known laws: the ratio of the distances to neighbouring rings remains constant and there is a power dependence between the distances to the rings and the time of their formation. The influence the electric field strength on the nature of the structures formed is investigated. It has been shown that an increase in the electric field strength leads to an increase in the number of structures formed if the electric field strength is positive and leads to a decrease in the number of structures formed if the electric field direction is opposite.

References

- [1] Liesegang R E 1896 Uber einige Eigenschaften von Gallerten *Naturwiss. Wochenschr.* **11**:353–362.
- [2] Keller J B and Rubinow S I 1981 Recurrent precipitation and Liesegang rings *J. Chem. Phys.* **74**:5000–5007.
- [3] Patankar S V 1980 Numerical heat transfer and fluid flow (Washington, DC: Hemisphere Publishing Corp.).
- [4] Lagzi I 2005 Liesegang patterns: Complex formation of precipitate in an electric field *Pramana – Journal of Physics* **64**(2):291-298.